

## Energy Levels of Chromium Ion Pairs in Ruby

P. KISLIUK\* AND N. C. CHANG\*

*The Aerospace Corporation, El Segundo, California 90245*

AND

P. L. SCOTT†

*The University of California, Santa Cruz, California 95060*

AND

M. H. L. PRYCE

*The University of British Columbia, Vancouver, British Columbia*

(Received 20 February 1969)

The lower energy levels of a number of transitions due to second-, third-, and fourth-nearest-neighbor chromium ion pairs in ruby are located by measuring the temperature dependence of optical absorption. Energy-level diagrams are constructed, from which many of the observed lines are identified. The measurements are consistent with earlier results for the ground states of first-, third-, and fourth-nearest-neighbor pairs. The ground-state levels of the second-nearest-neighbor pairs are describable by the isotropic exchange interaction  $H = J_2 \mathbf{S}_1 \cdot \mathbf{S}_2 + j_2 (\mathbf{S}_1 \cdot \mathbf{S}_2)^2$  with  $J_2 = 83.6 \text{ cm}^{-1}$  and  $j_2 = -9.7 \text{ cm}^{-1}$ , where  $\mathbf{S}_1$  and  $\mathbf{S}_2$  are the total spins of each of the two chromium ions. Description of the optically excited states requires a more general expression for the exchange interaction, of the form  $H = \sum J_{ij} \mathbf{s}_{1i} \cdot \mathbf{s}_{2j}$ , where  $\mathbf{s}_{1i}$  and  $\mathbf{s}_{2j}$  are the spins of electrons occupying the various one-electron orbitals on ions 1 and 2. The ground-state coupling parameters for the first four nearest-neighbor types are used to estimate the Néel and Curie-Weiss temperatures for  $\text{Cr}_2\text{O}_3$ .

### I. INTRODUCTION

THE  ${}^4A_2$  ground state and the  ${}^2E$  lowest excited state are the terminal levels of the well-known  $R_1$  and  $R_2$  lines of chromium ions in ruby.<sup>1,2</sup> In relatively concentrated samples ( $\sim 0.5\%$ ), many additional lines are observed in this region.<sup>3,4</sup> The spectrum at  $77^\circ\text{K}$  is shown in Fig. 1. These lines are due to interacting pairs of chromium ions.<sup>5,6</sup> Here, we are concerned only with those pairs of chromium ions in the four most closely spaced types of neighboring sites—one nearest neighbor, three equivalent second neighbors, three equivalent third neighbors, and six equivalent fourth neighbors.<sup>7</sup> These are the sites in the sapphire lattice connected by one or more Al—O—Al bonds. Beginning with fifth-neighbor pairs, at least two oxygen ions intervene. Thus, the exchange couplings of fifth- and further-neighbor pairs are so small that they give rise to a high density of transitions very close to the  $R$  lines; the first four neighbor pairs give well resolved transitions.

The low-lying levels (both ions in the  ${}^4A_2$  electronic state) that have been assigned to pairs in particular

relative positions are well accounted for by an exchange-type interaction Hamiltonian,  $H = J\mathbf{S}_1 \cdot \mathbf{S}_2$ , where  $\mathbf{S}_1$  and  $\mathbf{S}_2$  are the total spins of ion 1 and ion 2, respectively.<sup>8-11</sup> The experimental fit can be improved by using a two-parameter equation justified by higher-order theory,<sup>9</sup>  $H = J\mathbf{S}_1 \cdot \mathbf{S}_2 + j(\mathbf{S}_1 \cdot \mathbf{S}_2)^2$ , but such refinement plays no role at this stage of the description. The excited state in which one of the paired ions is raised to the  ${}^2E$  state has been treated theoretically on a similar basis<sup>12,13</sup>; the calculation is more difficult because the trigonal-field-spin-orbit splitting of the isolated  $\text{Cr}^{3+}$  ion ( $29 \text{ cm}^{-1}$ ) is, in this case, of the same order as the exchange coupling, and therefore must be considered simultaneously. The correspondence between experiment and this theory is poor; therefore, assignment of the observed excited

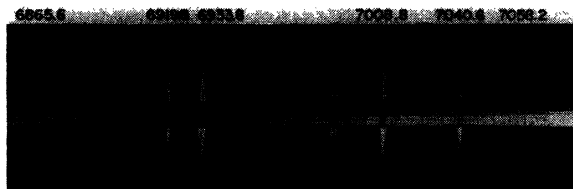


FIG. 1. Spectrum of 0.5% ruby, 5 cm long, at  $77^\circ\text{K}$ , mixed polarization. The center is in absorption, surrounded above and below by emission. The outermost spectrum is a neon spectral lamp wavelength reference.

\* Work supported by the U. S. Air Force under Contract No. F04701-68-C-0200.

† Work partially supported by the Office of Naval Research.

<sup>1</sup> S. Sugano and Y. Tanabe, *J. Phys. Soc. Japan* **13**, 880 (1958).

<sup>2</sup> S. Sugano and I. Tsujikawa, *J. Phys. Soc. Japan* **13**, 899 (1958).

<sup>3</sup> O. Deutschbein, *Ann. Physik* **14**, 712 (1932) and *Z. Physik* **77**, 489 (1934).

<sup>4</sup> S. F. Jacobs, doctoral thesis, The Johns Hopkins University, Baltimore, Maryland, 1956 (unpublished).

<sup>5</sup> A. L. Schawlow, D. L. Wood, and A. M. Clogston, *Phys. Rev. Letters* **3**, 502 (1959).

<sup>6</sup> N. A. Tolstoi and A. P. Abramov, *Opt. i Spektroskopiya* **14**, 691 (1963) [English transl.: *Opt. Spectry.* (USSR) **14**, 365 (1963)].

<sup>7</sup> An excellent figure showing the geometric relations of these pairs is given in N. Laurance, E. C. McIrvine, and J. Lambe, *J. Phys. Chem. Solids* **23**, 515 (1962).

<sup>8</sup> P. Kisliuk, A. L. Schawlow, and M. D. Sturge, *Advances in Quantum Electronics* (Columbia University Press, New York, 1964), p. 725.

<sup>9</sup> P. Kisliuk and W. F. Krupke, *Appl. Phys. Letters* **3**, 215 (1963).

<sup>10</sup> P. Kisliuk and W. F. Krupke, *J. Appl. Phys.* **36**, 1025 (1965).

<sup>11</sup> L. F. Mollenauer and A. L. Schawlow, *Phys. Rev.* **168**, 309 (1968).

<sup>12</sup> A. M. Clogston (unpublished).

<sup>13</sup> A. E. Nikiforov and V. I. Cherepanov, *Phys. Status Solidi* **14**, 391 (1966).

states to theoretical levels within this framework is not possible.<sup>10</sup> We now recognize that this difficulty in interpretation arises because a Hamiltonian of the above form is justified only if the electron spins are parallel and form a half-filled orbital electronic state in the octahedral approximation to the crystal field.<sup>14,15</sup> This condition is not fulfilled for the  ${}^2E$  state. Therefore, a more general approach must be used for the excited state of the pairs. A more general exchange Hamiltonian is of the form  $H = \sum J_{ij} \mathbf{s}_{1i} \cdot \mathbf{s}_{2j}$ , where  $s_1$  and  $s_2$  are the spins of electrons on ion 1 and ion 2, respectively, and  $i$  and  $j$  run over the three one-electron  $t_{2g}$  orbitals on each ion. Calculations based on this model have now been carried out,<sup>15</sup> and the problem of assigning experimentally observed lines to particular neighbor pairs and identifying energy levels now assumes new interest.

## II. EXPERIMENTAL

### A. Spectrum of Concentrated Ruby

The most detailed tabulation of the observed spectral lines in concentrated ruby is given by S. F. Jacobs.<sup>4</sup> We adopted his 77°K data for the purpose of listing energy levels, since precise levels depend on concentration and temperature. Jacobs kindly lent us the rubies used in his work, and we determined the concentration to be  $0.31 \pm 0.05\%$  of the aluminum ions replaced by chromium ions. Our own measurements were made on 0.5% samples in which the transitions were shifted to higher energy by about  $0.2 \text{ cm}^{-1}$ , and were somewhat broadened. Jacobs lists 110 resolved transitions in the region from 6850 to 7065 Å.

Several techniques are useful in assigning the transitions to particular pairs. The lines due to paired chromium ions can be distinguished from single-ion vibronic transitions by the concentration dependence of their intensity.<sup>5,6</sup> Fourth-neighbor pairs can be distinguished from the other neighbor pairs by their splitting in an axial electric field.<sup>16</sup> Comparison of optical results with microwave results<sup>17-20</sup> is also helpful in assigning the transitions; however, the most successful technique for

<sup>14</sup> J. H. Van Vleck, *Rev. Mat. y Fisica Teorica, Univ. Nac. de Tucuman, Argentina* **14**, 189 (1962).

<sup>15</sup> M. H. L. Pryce (to be published).

<sup>16</sup> A. A. Kaplyanskii, V. N. Medvedev, and A. K. Przewuskii, *Zh. Eksperim i Teor. Fiz. Pis'ma v Redaktsiyu* **5**, 427 (1967) [English transl.: *Soviet Phys.—JETP Letters* **5**, 347 (1967)], augmented by private communication from Kaplyanskii. It is verified that the following transitions of Table II split in an axial electric field as fourth-nearest-neighbor lines are expected to: 4I2, 4H2, 4G2, 4F2, 4F1, 4F0, 4D3, 4C3, 4E2, 4C2, 4A3, 4C1, 4A2, 4A1, 4B0, and 4A0. Lines due to the other three types of pairs should not split, and this behavior is verified for 3I1, 3H1, 3I2, 3D1, and 3C1.

<sup>17</sup> M. J. Weber, G. A. DeMars, and G. F. Koster, *Phys. Rev. Letters* **4**, 125 (1960).

<sup>18</sup> H. Statz, L. Rimai, M. J. Weber, G. A. DeMars, and G. F. Koster, *J. Appl. Phys. Suppl.* **32**, 218S (1961).

<sup>19</sup> H. Statz, M. J. Weber, L. Rimai, G. A. DeMars, and G. F. Koster, *J. Phys. Soc. Japan Suppl. B-1* **17**, 430 (1962).

<sup>20</sup> Yu. L. Shelekhin, M. P. Voltinov, and B. P. Bersovskii, *Fiz. Tverd. Tela* **8**, 589 (1966) [English transl.: *Soviet Phys.—Solid State* **8**, 469 (1966)].

ANTIFERROMAGNETIC COUPLING			FERROMAGNETIC COUPLING		
$H_{\text{EXCH}} = J(\vec{S}_1 \cdot \vec{S}_2)$			$H_{\text{EXCH}} = -J(\vec{S}_1 \cdot \vec{S}_2)$		
$Z_0 = 1 + 3e^{-J/kT} + 5e^{-3J/kT} + 7e^{-6J/kT}$			$Z_f = 7 + 5e^{-3J/kT} + 3e^{-5J/kT} + e^{-6J/kT}$		
ENERGY	$S =  \vec{S}_1 + \vec{S}_2 $	TEMP DEP	ENERGY	$S =  \vec{S}_1 + \vec{S}_2 $	TEMP DEP
6J —	3	$\frac{e^{-6J/kT}}{Z_0}$	6J —	0	$\frac{e^{-6J/kT}}{Z_f}$
3J —	2	$\frac{e^{-3J/kT}}{Z_0}$	5J —	1	$\frac{e^{-5J/kT}}{Z_f}$
J —	1	$\frac{e^{-J/kT}}{Z_0}$	3J —	2	$\frac{e^{-3J/kT}}{Z_f}$
0 —	0	$\frac{1}{Z_0}$	0 —	3	$\frac{1}{Z_f}$

FIG. 2. Energy levels and temperature dependence of the population of exchange-coupled pairs of ions in the quartet orbital electronic state.

identifying the kind of pair has been the response to uniaxial stress.<sup>11,21,22</sup> The problem of extracting the energy levels from the transitions assigned to a particular neighbor pair can be attacked by the temperature dependence of absorption<sup>8,9,11</sup> and of emission,<sup>23</sup> and by monochromatic excitation,<sup>24</sup> as well as by finding recurring differences in the observed transition energies. We used the temperature dependence of absorption to assign certain transitions that were, in turn, helpful in determining recurring differences. After considering all available sources of information, we were able to assign most of the transitions observed by Jacobs<sup>4</sup> to particular energy levels.

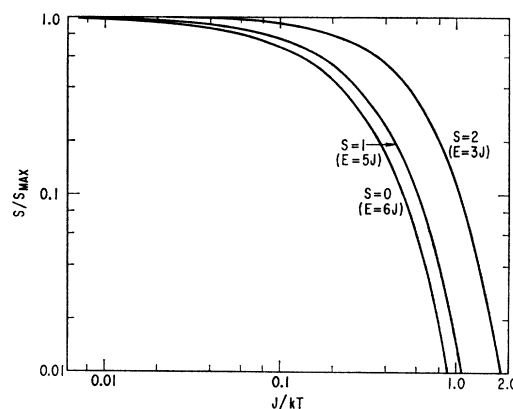


FIG. 3. Plot of the expressions from Fig. 2 for ferromagnetically coupled pairs.

<sup>21</sup> A. A. Kaplyanskii and A. K. Przewuskii, *Dokl. Akad. Nauk SSSR* **142**, 313 (1962) [English transl.: *Soviet Phys.—Doklady* **7**, 37 (1962)].

<sup>22</sup> A. A. Kaplyanskii and A. K. Przewuskii, *Fiz. Tverd. Tela* **9**, 257 (1967) [English transl.: *Soviet Phys.—Solid State* **9**, 190 (1967)].

<sup>23</sup> R. C. Powell, B. DiBartolo, B. Birang, and C. S. Naiman, *Phys. Rev.* **155**, 296 (1967). Note that our assignment of the 6927-Å line differs from that of these authors.

<sup>24</sup> R. T. Daly, Paper TB16 presented at meeting of the Optical Society of America held at Pittsburgh, Pennsylvania (1961).

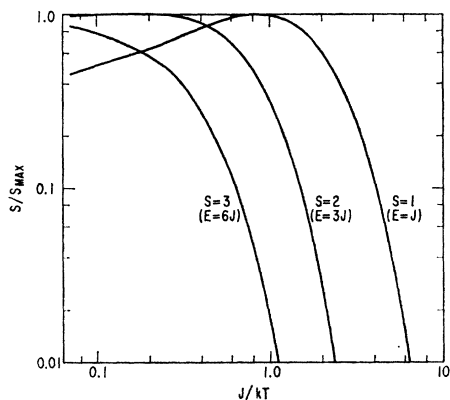


FIG. 4. Plot of the expressions from Fig. 2 for antiferromagnetically coupled pairs.

### B. Temperature Dependence of Absorption

We assumed that in the temperature range of our experimentation, the strength of the temperature dependence of absorption is due to the change in population of the initial electronic state; i.e., that changes in the occupation of the vibrational modes do not appreciably affect the intensities of these "no-phonon" lines. By assuming the  $H = JS_1 \cdot S_2$  form of interaction Hamiltonian, and ignoring the  $0.38\text{-cm}^{-1}$  splitting of the ground state as negligible in comparison with the exchange splitting, we obtained the predicted temperature dependence shown in Figs. 2-4. In earlier work, the integrated absorption intensities of the two strongest pair lines led to the identification of two types of pairs, with  $J = 11.4$  and  $-7.4\text{ cm}^{-1}$ .<sup>9,10</sup> These have now been definitely identified with third and fourth nearest neighbors, respectively.<sup>11,22</sup> The present work extends this technique to as many of the lines as can be seen with sufficient intensity in absorption. Because of difficulties with the many partially resolved lines, only peak (rather than integrated) intensities were measured. The linewidth did not change noticeably over the temperature range used,  $4\text{-}77^\circ\text{K}$ . The background due to neighboring lines was extrapolated visually. Absorption measurements were made using a 1-m Jarrell-Ash

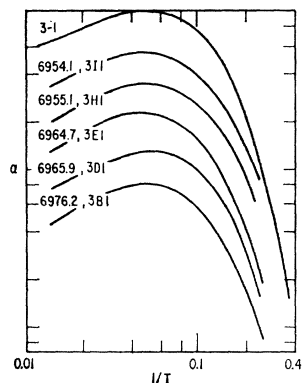


FIG. 5. Temperature dependence of absorption strength for lines originating on the third neighbor  $S=1$  level. The upper curve is the theoretical curve for the energy levels given in Table I. The designation of the lines conforms to that given in Table II.  $1/T$  is in  $^\circ\text{K}^{-1}$ .

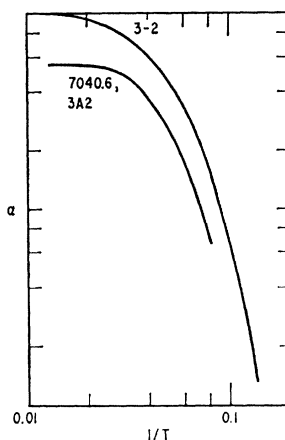


FIG. 6. Temperature dependence of absorption strength for lines originating on the third-neighbor  $S=2$  level. The upper curve is the theoretical curve for the energy levels given in Table I. The designation of the lines conforms to that given in Table II.  $1/T$  is in  $^\circ\text{K}^{-1}$ .

grating spectrometer in eighth order; higher orders were eliminated with suitable Corning filters and lower orders by the response of the RCA 7265 photomultiplier tube. The crystal was mounted on a large copper block and allowed to warm slowly from  $4^\circ\text{K}$ . Temperature measurements were made using a calibrated carbon resistor mounted in the copper block. The results of these measurements are summarized in Figs. 5-8.

Based on these and previously published results, we constructed the energy levels given in Table I and Fig. 9, and obtained the agreement with experiment shown in Table II.

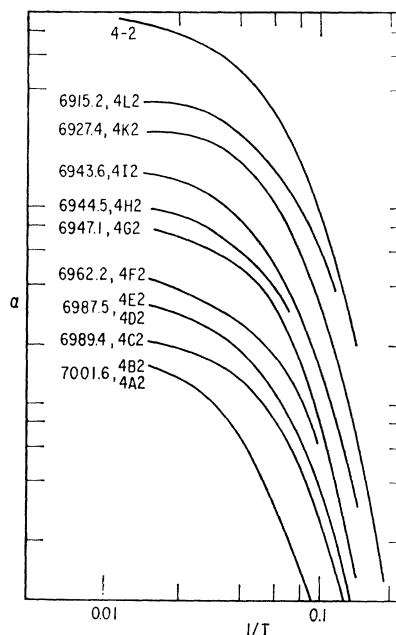


FIG. 7. Temperature dependence of absorption strength for lines originating on the fourth-neighbor  $S=2$  level. The upper curve is the theoretical curve for the energy levels given in Table I. The designation of the lines conforms to that given in Table II.  $1/T$  is in  $^\circ\text{K}^{-1}$ .

### III. DISCUSSION AND RESULTS

#### A. Fine Structure in the Ground Levels

The  $0.38\text{-cm}^{-1}$  crystal-field-spin-orbit splitting of the isolated ion  ${}^4A_2$  ground state can be described by a term in the spin Hamiltonian of the form  $DS_z^2$ . An investigation of the contribution of this term, as well as small amounts of anisotropic exchange and dipolar interaction, to the ground-state levels of the fourth-nearest-neighbor pair system shows that such terms introduce splittings of fractions of  $1\text{ cm}^{-1}$ , within the levels characterized by a total spin  $S$ .<sup>25</sup> For example, the  $7009\text{-\AA}$  line in a dilute sample shows structure that arises, in part, from such terms.<sup>26</sup> In the somewhat more concentrated samples used by Jacobs, and by us, this structure is generally not resolved. Therefore, it is not included in Table I, and is included in Table II only in the one instance where it appears to be resolved.

#### B. Fine Structure in the Excited Levels

Splitting of the isolated ion  ${}^2E$  state is  $29\text{ cm}^{-1}$ ; therefore, it is not obvious that this interaction is sufficiently small to be treated by perturbation theory, as was done above in the case for the ground state. Nevertheless, if the exchange splitting is appreciably larger than  $29\text{ cm}^{-1}$ , the total spin of the excited state becomes a reasonably good quantum number (with values 1 and 2), and perturbation theory becomes a valid approximation. A result of such a calculation is

TABLE I. Best-fit energy levels ( $\text{cm}^{-1}$ ).

Ground state		Excited state	
Fourth neighbors			
$S=3$	0	A	14,298.7
2	20.4	B	299.4
1	35.1	C	324.1
0	43.2	D	327.2
		E	328.2
		F	379.9
		G	411.2
		H	416.2
		I	418.2
		J	446.0
		K	451.8
		L	477.5
Third neighbors			
$S=0$	0	A	14,233.1*
1	11.3	B	341.8
2	33.9	C	344.2
3	69.0	D	363.2
		E	365.5
		F	378.5
		G	380.9
		H	385.2
		I	387.5

\* Double,  $\Delta=1.1\text{ cm}^{-1}$ ; Ref. 26; and G. F. Imbusch (private communication).

<sup>25</sup> M. J. Berggren, G. F. Imbusch, and P. L. Scott, *Bull. Am. Phys. Soc.* **13**, 1659 (1968).

<sup>26</sup> A. L. Schawlow, *J. Appl. Phys. Suppl.* **33**, 395 (1962).

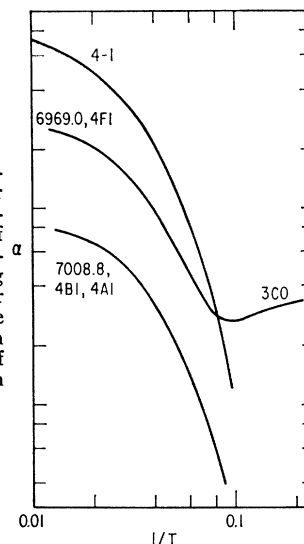


FIG. 8. Temperature dependence of absorption strength for lines originating on the fourth-neighbor  $S=1$  level, one of which is an unresolved composite with a level originating on the ground state. The upper curve is the theoretical curve for the energy levels given in Table I. The designation of lines conforms to that given in Table II.  $1/T$  is in  ${}^\circ\text{K}^{-1}$ .

that the intervals between the three levels of  $S=2$  are in a 3-to-1 ratio.<sup>15</sup> As shown in Fig. 9, this appears true whenever the levels in question are resolved.

#### C. First- and Second-Neighbor Pairs

We have shown that almost all of the complicated spectrum illustrated in Fig. 1 and reported by Deutschein<sup>3</sup> and Jacobs<sup>4</sup> is due to third, fourth, and more distant neighbors. The first-neighbor lines are sparse partly because there are statistically fewer such pairs, but other factors also reduce the number of observed transitions due to the two closest neighbor pairs. For their relatively large exchange couplings, only the ground state is appreciably populated below  $77^\circ\text{K}$  in absorption measurements, and only the lowest of the metastable excited levels in emission measurements. In addition, the  $S=0$  ground state in these antiferromagnetically coupled pairs results in restrictive selection

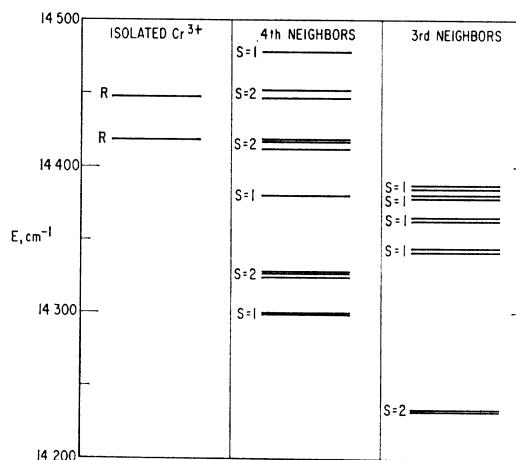


FIG. 9. Excited-state energy levels of third and fourth nearest neighbors.

TABLE II. Comparison of spectrum predicted from energy levels of Table I with that observed by Jacobs (Ref. 4) (all  $\bar{\nu}$  in  $\text{cm}^{-1}$ ).<sup>a</sup>

Assignment	$\bar{\nu}$ Calc.	Observed absorption spectrum								Observed emission spectrum			
		$\bar{\nu}_1$ (77°K)	$I$ (77°K)	$\bar{\nu}_{11}$ (77°K)	$I$ (77°K)	$\bar{\nu}_1$ (4°K)	$I$ (4°K)	$\bar{\nu}_{11}$ (4°K)	$I$ (4°K)	$\bar{\nu}$ (77°K)	$I$ (77°K)	$\bar{\nu}$ (4°K)	$I$ (4°K)
2		14,590.03	0d <sub>1</sub>			14,590.34	0dd						
2								14,587.79	0dd				
2		561.32	3			561.68	4						
4L3	14,477.5					477.82	0d						
		464.19	1d										
										14,461.59	1		
										461.14	0		
										458.97	0		
4L2	457.1	456.88	0d	14,456.94	1d					457.00	1		
Dist						455.68	0			456.24	1		
Dist						455.12	2	454.95	0	454.80	1		
Dist		454.10	1			454.46	2			454.05	1		
Dist		452.64	1			452.97	3			452.60	0		
4K3	451.8	451.80	1			451.98	4						
Dist				451.10	3			451.45	3				
Dist		450.76	4			450.94	6			450.65	5		
R		447.23	10	447.13	10	447.36	10	447.70	10	446.96	10		
Dist		443.67	2d			444.02	3			443.79	0		
Dist										443.46	0		
Dist		442.58	2			442.90	3			442.54	0		
Dist		442.05	2			442.30	3			441.96	0		
Dist		440.55	2	440.34	1d	440.94	3	440.66	1d	440.61	0		
Dist		439.84	2			440.25	3			439.70	0		
Dist		438.78	2	438.75	1d	439.08	3 <sub>1</sub>			438.76	0		
Dist		438.22	2			438.49	3			438.06	0		
Dist		437.35	0							437.26	0		
Dist		436.51	0							436.50	0		
Dist		435.72	0							435.64	0		
4K2	431.4	431.40	4	431.38	5					431.28	5d		
4J2	425.6	425.58	4	425.57	5	425.89	2			425.47	6d		
Dist						424.79	2						
Dist						423.22	2						
Dist		422.60	6	422.20	5	422.12	4	421.98	2	421.60	7d	421.96	4d
R		418.16	10	417.63	10	418.52	10	418.19	10	417.83	10	418.42	10
Dist										414.02	3	414.34	1
Dist		413.03	2							412.96	3	413.14	2
4G3	411.2	411.51	2	411.53	1d			411.82	1	411.30	3		
Dist		410.60	2			411.04	6			410.49	4	410.80	2d
Dist		409.83	2							410.03	4		
Dist		408.95	2			409.27	3			408.92	3	409.35	2d
Dist		407.76	2			408.05	3			407.66	3	408.02	2d
Dist		406.26	0							406.11	2	406.71	0
Dist										404.9 <sup>b</sup>	0		
4I2	397.8	397.76	2	397.77	2					397.72	3		
4H2	395.9	395.82	2	395.90	4					395.74	4		
4G2	390.8	390.48	3	390.55	4					390.46	3		
		388.59	1										
3I0	387.5	387.50	0			387.84	4	387.80	4				
4I1	383.1		(obs)				(obs)			383.03	0		
3G0	380.9		(obs)			381.68	0d			381.06	0		
4F3	379.9		(obs)				(obs)			379.56	0		
3I1	376.2	376.05	4	376.15	4	376.36	0	376.36	1d	375.96	1		
3H1	373.9	374.05	3	374.04	1	374.35	0		(obs)	373.86	1d		
4H0	373.0			373.58	1				(obs)				
3G1	369.6	369.8 <sup>b</sup>	0										
3F1	367.2	367.24	0							367.19	0		
3E0	365.5	365.56	0			365.84	4			365.44	0		
3D0	363.2	363.22	0			363.53	4d	363.66	0	363.13	0		
4F2	359.5	359.35	4	359.22	2d					359.28	6		
3E1	354.2	354.10	0d							354.27	0		
3I2	353.6	353.35	0							353.22	0		
3D1	351.9	351.72	0							351.54	0		
4F1	344.8								(obs)	344.49	7		
3C0	344.2	344.55	4d	344.17	4	344.31	2						
3B0	341.8		(obs)			342.24	0						
4F0	336.7	336.77	0										
3C1	332.9	333.05	2				(obs)			336.88	2		
3B1	330.5	330.51	4			333.30	0			332.92	2		
4E3	328.2	328.10	2d			330.79	1			330.42	3		
4D3	327.2	327.13	2d			328.43	2			328.00	2		
						327.51	2			327.03	4		

TABLE II (continued)

Assign- ment	p Calc.	Observed absorption spectrum						Observed emission spectrum					
		$\bar{\nu}_1$ (77°K)	$I$ (77°K)	$\bar{\nu}_{11}$ (77°K)	$I$ (77°K)	$\bar{\nu}_1$ (4°K)	$I$ (4°K)	$\bar{\nu}_{11}$ (4°K)	$I$ (4°K)	$\bar{\nu}$ (77°K)	$I$ (77°K)	$\bar{\nu}$ (4°K)	$I$ (4°K)
4C3	324.1	324.30	2d			324.62	3			324.19	7		
4C3 (G.S.)		323.85	1				(obs)				(obs)		
4E2	307.8	307.85	2	307.88	3					307.70	6		
4D2	306.8	306.85	2	306.80	3					306.66	7		
4C2	303.7	303.47	2	303.49	4					303.39	7	303.54	0
4B3	299.4					299.61	1d						
4A3	298.7					298.88	1d			298.68	2	299.01	3
2		293.89	5d			294.28	5d	294.15	0d	293.63	2		
4D1	292.1	291.98	1d	291.94	0d					291.85	4		
4C1	289.0						(obs)			288.31	0		
4E0	285.0						(obs)			285.41	0		
4D0	284.0						(obs)			284.28	0		
4B2	279.0	278.81	1d				°			278.54	7	278.62	7 <sup>d</sup>
4A2	278.3	278.09	1d				°						
										267.27 <sup>°</sup>	0d		
{4B1	264.3 <sup>f</sup>												
{4A1	263.6 <sup>f</sup>	263.82	4	263.78	5					263.66	10	263.92	9
4B0	256.2									256.38	3	256.07	3
4A0	255.5									255.55	3		
2		231.99	0d <sup>g</sup>								(obs)		
3A1	221.8									221.68	1dd		(obs)
3A2	199.2	199.31	5d							199.17	9d	199.33	8d
Vib											(obs)	189.8	1d
Vib											(obs)	180.5	1d
Vib										169.4	1d	168.1	1d
3A3	164.1									164.1	2d	164.9	2d
Vib											(obs)	152.4	1d

<sup>a</sup> Dist = due to neighbors more distant than the fourth, R = one of the two R lines due to isolated Cr<sup>3+</sup> ions, Vib = Vibronic satellites of R lines, 2 = due to second neighbors, 4A3, 3A0, etc. = fourth or third neighbor pairs, respectively, transition between excited level A and ground state S = 3 or S = 0, re- spectively, G. S. = resolved structure due to ground-state spin-orbit splitting, (obs) = seen but too weak to measure, d = diffuse, dd = very diffuse.

<sup>b</sup> Our observation; not in Jacobs' table.

<sup>c</sup> Although not listed at 4°K by Jacobs, present and only moderately diminished from its 77°K intensity.

<sup>d</sup> Intensity listed as 2 by Jacobs; obviously a typographical error.

<sup>e</sup> Although it is not so close to any other line that we might have failed to resolve it, we did not observe this line.

<sup>f</sup> These two lines resolved by Schawlow; Ref. 26.

<sup>g</sup> Double line, poorly resolved.

rules in absorption. At higher temperatures, the greatly broadened lines and the appearance of the anti-Stokes vibronic spectrum make absorption measurements very difficult. In emission, the major portion of these pair

lines lies in the same region as the vibronic sidebands of the R lines, even at low temperature. Despite the difficulties expressed above, experimental progress has been made by using a longer, more concentrated ruby

TABLE III. Second-nearest-neighbor lines.

Wavelength	Uniaxial stress splitting	Absorption	Emission
7452	Refs. 11, 22	Disappears with lowering temperature as $e^{-\Delta/kT}$ with $\Delta \sim 590 \text{ cm}^{-1}$	Present 4°K
7290 <sup>11,22</sup>	About one-half that of 7452	$\Delta \sim 300 \text{ cm}^{-1}$	Appears to remain down <sup>a</sup> to 23°K <sup>a</sup>
7282	About one-half that of 7452	$\Delta \sim 300 \text{ cm}^{-1}$	Appears to remain down to 23°K <sup>a</sup>
7214 <sup>11,22</sup>	About one-fourth that of 7452	Disappears at low temperature	Present 4°K
7159 <sup>11</sup>	About one-fourth that of 7452	$\Delta \sim 140 \text{ cm}^{-1}$	Disappears at low temperature
7119		$\Delta \sim 140 \text{ cm}^{-1}$	Appears to remain down to 23°K <sup>a</sup>
7092	About one-fourth that of 7452	Present at 4°K, weakens with increasing temperature in reasonable agreement with 2nd <i>nn</i> calculated partition function.	Disappears at low temperature
7024		$\Delta \sim 140 \text{ cm}^{-1}$	Not observed
6994		Like 7092	Disappears at low temperature <sup>]</sup>
6912		$\Delta \sim 140 \text{ cm}^{-1}$ (very crude)	Not observed
6865		Like 7092	Not observed
6853		Like 7092	Not observed
6852		Like 7092	Not observed

<sup>a</sup> Identification of emission line as the same transition as absorption questionable—may be vibronic.

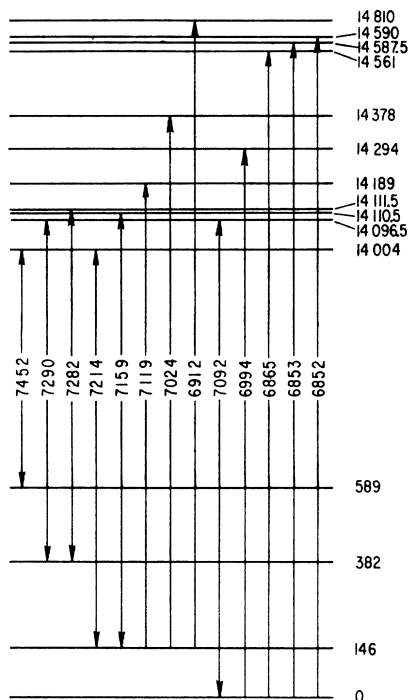


FIG. 10. Energy levels of second nearest neighbors.

(15 cm,  $\sim 1\%$ ) and modern signal-averaging techniques. Uniaxial stress behavior also has been used to identify neighbor pairs.<sup>11,22</sup>

We can add nothing to the published work on first neighbors,<sup>11,22</sup> but new results have been obtained for second neighbors. A center of inversion symmetry lies between the ions of this pair<sup>15,27</sup>; therefore, the states can be classified odd or even under inversion. Because the low-lying levels of the pair are made up of the same orbitally nondegenerate state on each ion, the parity of these levels is uniquely associated with the total spin. In the excited state, on the other hand, both parities occur with each of the two possible values of the spin. The electric dipole selection rule then results in the division of the transitions into two groups, with no energy level common to both. Thus, the positions of some of the levels cannot be determined from spectral intervals alone, and are placed in this work only by the temperature dependence of absorption.

Table III is a summary of the experimental results on those spectral lines that we associate with second nearest neighbors. Uniaxial stress splitting is similar in pattern for all of the lines in Table III for which it has been observed; it differs in magnitude as indicated. A plausible energy level diagram derived from these results is shown in Fig. 10. The low-lying levels can be fitted by a Hamiltonian of the form  $H = J(\mathbf{S}_1 \cdot \mathbf{S}_2)$

<sup>27</sup> S. V. Vonsovskii, V. I. Cherepanov, A. N. Men, and A. E. Nikiforov, *Phys. Status Solidi* **24**, 51 (1967).

+  $j(\mathbf{S}_1 \cdot \mathbf{S}_2)^2$ , where  $J = 83.6 \text{ cm}^{-1}$  and  $j = -9.7 \text{ cm}^{-1}$ ; the relatively large ratio  $j/J$  is justified by the low-frequency "accordion" mode of vibration that strongly affects this exchange.

#### IV. GENERAL COMMENTS

Transitions from the ground level to the remaining low-lying levels of different spin are forbidden in first order for both electric and magnetic dipole transitions. The far-infrared spectrum should, therefore, be very weak, and reports of direct observations of these transitions are probably erroneous.<sup>28,29</sup>

When the observed ground-state exchange parameters for the four nearest neighbors in ruby are used to calculate the Curie-Weiss temperature for a hypothetical  $\text{Cr}_2\text{O}_3$  crystal with these couplings by the molecular field method, a value of  $\theta = 840^\circ\text{K}$  is obtained, compared with the experimentally measured value of  $550^\circ\text{K}$  for  $\text{Cr}_2\text{O}_3$ .<sup>30</sup> When the Néel temperature is similarly calculated,<sup>31,32</sup> one obtains  $T_N = 980^\circ\text{K}$  by the simple molecular field method and  $838^\circ\text{K}$  by the Oguchi method, compared with the experimental value of  $310^\circ\text{K}$  for  $\text{Cr}_2\text{O}_3$ .<sup>33</sup> These discrepancies occur because the lattice parameters for  $\text{Cr}_2\text{O}_3$  are about 4% larger than for  $\text{Al}_2\text{O}_3$ .<sup>34</sup> In addition, little data exists on first nearest neighbors, and the exchange parameter ( $J_1 \approx 240 \text{ cm}^{-1}$ ) is known only within about 20%. The relative values of these ruby pair parameters are useful in estimating which pairs must be included to give a realistic theory of  $\text{Cr}_2\text{O}_3$  magnetism. The two nearest-neighbor pairs (one first neighbor with  $J \sim 240 \text{ cm}^{-1}$ <sup>11</sup> and three second neighbors with  $J \sim 84 \text{ cm}^{-1}$ ) are sufficient to determine the type of spin-ordering at low temperature and to calculate the Curie-Weiss and Néel temperatures to a precision of  $\pm 20\%$ . Since changing the sign of the fourth-neighbor interaction would not be sufficiently strong to change the low-temperature spin ordering, the argument of Osmund<sup>35</sup> to account for the different ordering in  $\text{Fe}_2\text{O}_3$  from that in  $\text{Cr}_2\text{O}_3$  is insufficient, even though he correctly predicted the sign of the coupling for fourth nearest neighbors. Neighbors more distant than the fourth are estimated to contribute no more than 3% to the magnetic properties of  $\text{Cr}_2\text{O}_3$ .

The attempt to assign the excited levels and extract the parameters of the more general exchange Hamiltonian will be considered in another paper.<sup>15</sup> We also

<sup>28</sup> A. Hadni, *Phys. Rev.* **136**, A758 (1964).

<sup>29</sup> J. F. Moser, H. Steffen, and F. K. Kneubuhl, *Helv. Phys. Acta* **39**, 195 (1966).

<sup>30</sup> G. Foex and M. Graff, *Compt. Rend.* **209**, 161 (1939).

<sup>31</sup> G. W. Pratt and P. T. Bailey, *Phys. Rev.* **131**, 1923 (1963).

<sup>32</sup> We are indebted to Dr. M. Tachiki and Dr. Malcolm Lines for independent computations of the Néel temperature.

<sup>33</sup> T. R. McGuire, E. J. Scott, and F. H. Grannis, *Phys. Rev.* **102**, 1000 (1956).

<sup>34</sup> R. E. Newnham and Y. M. DeHaan, *Z. Krist.* **117**, 235 (1962).

<sup>35</sup> W. P. Osmund, *Proc. Phys. Soc. (London)* **79**, 394 (1962).

expect the more general Hamiltonian

$$H = \sum J_{ij} \mathbf{s}_{1i} \cdot \mathbf{s}_{2j}$$

to be required in the case of  $Mn^{++}$  pairs in  $ZnS:MnS$ , where experimental results have been analyzed on the basis of the simple exchange Hamiltonian.<sup>36</sup> In this case, also, the order of the spin levels in the excited state appears to be opposite to that in the ground state in the

<sup>36</sup> D. S. McClure, *J. Chem. Phys.* **39**, 2850 (1963).

sense that a high-spin level lies lowest in the metastable excited state, whereas the low-spin level lies lowest in the ground state.

#### ACKNOWLEDGMENTS

The authors would like to thank Dr. R. L. Orbach, Dr. M. Tachiki, and Dr. N. L. Huang for helpful discussions, J. H. Whang for able technical assistance, and Dr. A. A. Kaplyanskii for unpublished experimental results.

### Nuclear Gamma-Ray Resonance Study of Hyperfine Interactions in $^{238}\text{U}^\dagger$

S. L. RUBY, G. M. KALVIUS, B. D. DUNLAP, G. K. SHENOY, D. COHEN,  
M. B. BRODSKY, AND D. J. LAM

*Argonne National Laboratory, Argonne, Illinois 60439*

(Received 7 February 1969)

Nuclear  $\gamma$ -ray resonance (the Mössbauer effect) has been observed in  $^{238}\text{U}$  using the 44.7-keV transition from the first excited state ( $2^+$ ) to the ground state ( $0^+$ ). The  $\gamma$  rays were obtained from the  $\alpha$  decay of  $^{242}\text{Pu}$ . The source material ( $\text{PuO}_2$ ) gave a single emission line having a width of about 40 mm/sec, which is roughly 1.5 times the natural linewidth. Absorption spectra were taken in the temperature region between 77 and 4.2°K using the following absorbers:  $\text{UO}_2$ , UC,  $\text{UF}_4$ ,  $(\text{UO}_2)(\text{NO}_3)_2 \cdot 6\text{H}_2\text{O}$ ,  $\text{UO}_3$ ,  $\text{UFe}_2$ , and  $\alpha$ -uranium metal. Several compounds showed partially resolved hyperfine spectra. In  $\text{UO}_2$  the resonance line broadens by a factor of 2 when cooling from 77 to 4.2°K. By fitting a pure magnetic hyperfine spectrum to the widened line, a hyperfine field of  $2700 \pm 200$  kOe was deduced, using  $g(2^+) = g_R = 0.25$ . The resonance in  $(\text{UO}_2)(\text{NO}_3)_2 \cdot 6\text{H}_2\text{O}$  can be explained by a pure electric quadrupole interaction of  $e^2qQ = -6100 \pm 225$  MHz. The isomer shift between  $\text{U}^{4+}$  and  $\text{U}^{6+}$  compounds is smaller than 2 mm/sec, thus giving a limit for the relative change in nuclear charge radius of  $|\delta\langle r^2 \rangle / \langle r^2 \rangle| \leq 10^{-8}$ .

#### I. INTRODUCTION

**N**UCLEI of the actinide elements fall into the second region of strong nuclear deformation ( $A \geq 220$ ). Because of the deformation, the lowest nuclear levels are collective in nature with rather small excitation energies. In particular, the rotational excitation energy is about 50 keV, and for this reason a large number of actinide nuclei are favorable isotopes for nuclear  $\gamma$ -ray resonance (Mössbauer-effect) experiments. However, a difficulty not encountered in other regions of the Periodic Table is that these nuclei are unstable, hence the absorbers will also be radioactive, and this limits substantially the number of possible candidates. The most favorable isotope for nuclear gamma-ray resonance (NGR) is the 59.6-keV resonance of  $^{237}\text{Np}$  ( $\tau_n = 63$  nsec), which to the present has been the only actinide isotope extensively studied. In that high-resolution case, detailed information can be obtained due to the large hyperfine interactions and the extremely large isomer shifts.<sup>1,2</sup>

<sup>†</sup> Based on work performed under the auspices of the U. S. Atomic Energy Commission.

<sup>1</sup> B. D. Dunlap, G. M. Kalvius, S. L. Ruby, M. B. Brodsky, and D. Cohen, *Phys. Rev.* **171**, 316 (1968).

<sup>2</sup> W. L. Pillinger and J. A. Stone, in *Mössbauer Effect Method-*

There is considerable interest in obtaining NGR spectra in  $^{238}\text{U}$  because of the widespread work on uranium systems by other techniques. The appropriate  $\gamma$  ray here comes from the  $0^+ \rightarrow 2^+$  transition at 44.7 keV.

As in all  $E2$  transitions, the lifetime is rather short (in this case 0.23 nsec). This results in relatively poor energy resolution as compared with most NGR isotopes. However, the internal fields were expected to be large in uranium, and it seemed worthwhile to attempt the resonance measurements.

Coulomb excitation provides one method for obtaining a source of the desired  $\gamma$  rays. However, in many cases the technique is not simple. We have failed during the last three years in attempts to observe NGR absorption in  $^{235}\text{U}$  using both 4-MeV  $\alpha$  particles and 35-MeV  $^{16}\text{O}$  bombardment ions, despite an abundance of 45-keV  $\gamma$  rays. The group at Johns Hopkins has been able to see the  $^{238}\text{U}$  resonance after Coulomb excitation with 3-MeV  $\alpha$  particles, and to observe some sign of hyperfine splitting.<sup>3</sup> Nonetheless, it is still quite desirable to find a radioactive source for the  $^{238}\text{U}$   $\gamma$  rays.

*ology*, edited by I. J. Gruverman (Plenum Press, Inc. New York, 1968), Vol. 4, pp. 217-236.

<sup>3</sup> J. R. Oleson, Y. K. Lee, J. C. Walker, and J. Wiggins, *Phys. Letters* **25B**, 258 (1967).

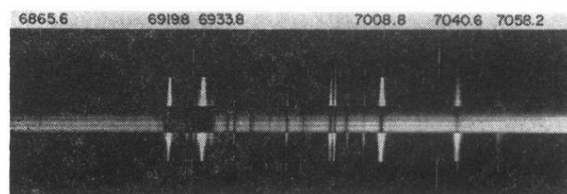


FIG. 1. Spectrum of 0.5% ruby, 5 cm long, at 77°K, mixed polarization. The center is in absorption, surrounded above and below by emission. The outermost spectrum is a neon spectral lamp wavelength reference.